

Nonuniversality of the non-Fermi-liquid state in $\text{CeRhSb}_{1-x}\text{Sn}_x$ compounds on the Sn-rich side

A. Ślebarski,¹ J. Spałek,² M. Gamża,¹ and A. Hackemer³¹*Institute of Physics, University of Silesia, 40-007 Katowice, Poland*²*Marian Smoluchowski Institute of Physics, Jagiellonian University, Reymonta 4, 30-059 Kraków, Poland*³*Institute for Low Temperature and Structure Research, Polish Academy of Sciences, 50-950 Wrocław, Poland*

(Received 20 November 2005; revised manuscript received 21 February 2006; published 22 May 2006)

We examine the electronic properties of the $\text{CeRhSb}_{1-x}\text{Sn}_x$ metallic series with $0.78 \leq x \leq 1$ by treating the *non-Fermi liquid* (NFL) state of CeRhSn as a reference state. A *nonuniversal* behavior of the NFL phase is observed as a function of x , which is attributed to enhanced magnetic disorder effects introduced by alloying, from one side and to the role of *spin fluctuations* due to Rh $4d$ electrons from the other. The NFL behavior at the lowest temperatures is attributed to quantum critical fluctuations among $4f$ electrons due to Ce, whereas the spin fluctuations become pronounced at higher temperatures $T > 6$ K. Thus, in Sn-rich samples those two types of fluctuations coexist. An itinerant-electron type of spin-glass-like state with a small magnetic moment appears at temperatures $T \leq 5$ K. These studies complement our previous work on the same system in the Sb-rich region, i.e., with $0 \leq x < 0.2$, where the *Kondo semiconducting state* evolves into *NFL state* via a quantum critical point located at $x \cong 0.12$.

DOI: 10.1103/PhysRevB.73.205115

PACS number(s): 71.27.+a, 72.15.Qm, 71.30+h

I. INTRODUCTION

CeRhSb represents a rare example of cerium-containing heavy-fermion (HF) Kondo insulator with a narrow energy gap ($2\Delta \cong 15$ K) in the electronic density of states (DOS).¹ The nonmagnetic and insulating state is gradually formed at temperatures below $T \sim 10$ K, whereas at higher temperatures it disappears.² The Kondo insulator (KI) discussed within the periodic Anderson model provides an insulating state for a \mathbf{k} -independent (intrasite) hybridization and for an even number of electrons per site;³ this is the case for CeRhSb . However, by changing the number of carriers, the gap should disappear even at temperature $T=0$. In this respect our previous alloying studies showed⁴ that the substitution of Sn atoms for Sb leads to the metallic behavior above the critical concentration $x_c \cong 0.12$ in the $\text{CeRhSb}_{1-x}\text{Sn}_x$ compounds. On the other hand, the compound CeRhSn displays a non-Fermi liquid character of the low-temperature physical properties,⁵ which were modeled in terms of the Griffiths phases.⁶ In this model, the combined effect of sufficiently strong disorder and the competition between the Kondo and the RKKY interactions can lead to a pocket of magnetically ordered regions (Griffiths phases⁶), where the order-parameter dynamics may determine thermodynamic properties of the system in the vicinity of a quantum critical point and is due to the tunneling between different configurations. Explicitly, it has been shown that the electrical resistivity increases as a function of the temperature as $\Delta\rho \propto T^\varepsilon$, with the exponent $\varepsilon \cong 1$, whereas both the quantity $C(T)/T$ related to the specific heat, $C(T)$, as well as the magnetic susceptibility, $\chi(T)$, vary as T^{-n} , with $n \cong 0.5$.⁵

In view of the diverse behavior of CeRhSb and CeRhSn compounds, it is of interest to examine in detail the solid solution $\text{CeRhSb}_{1-x}\text{Sn}_x$, to see the effect of the decreasing number of conduction electrons on the gap formation in CeRhSb , as well as on the changes in the metallic ground-state properties across the series. The x -ray diffraction stud-

ies showed, however, that the $\text{CeRhSb}_{1-x}\text{Sn}_x$ compounds exist in the limited Sn-concentration regimes. Namely, the samples are single-phase only for either $x \leq 0.2$ (with orthorhombic ϵ - TiNiSi structure, space group $Pnma$) or for $x \geq 0.8$ (with hexagonal of the Fe_2P structure type, space group $P\bar{6}2m$).⁷ On the Sb-rich side ($0 \leq x \leq 0.2$), we have observed very recently⁴ the transition: *Kondo insulator* \rightarrow *non-Fermi liquid* as a function of the number of carriers. Namely, the system undergoes the nonmagnetic Kondo insulator-magnetic metal transition via a quantum critical point located at $x \cong 0.12$.⁴ On the metallic side, a quantum critical behavior has been discovered for samples with $x \rightarrow 0.12$ from above, that is specified by the power law for the resistivity, the susceptibility, and the specific heat. This quantum critical behavior is associated with the localization of correlated electrons in this hybridized system. We have also observed a universal scaling between the electrical resistivity and the magnetic susceptibility in the form $\rho\chi = \text{const}$, in the quantum-coherence regime for the Kondo semiconductors $\text{CeRhSb}_{1-x}\text{Sn}_x$, with $x \leq 0.12$.⁴

The purpose of this paper is to discuss in detail and to interpret, at least qualitatively, the quantum behavior for the Sn-rich samples ($x \geq 0.8$) of $\text{CeRhSb}_{1-x}\text{Sn}_x$ compounds. As mentioned above, CeRhSn is a non-Fermi liquid.⁵ In the solid solutions $\text{CeRhSb}_{1-x}\text{Sn}_x$, resistivity $\rho(T)$ exhibits different types of behavior;⁷ namely $\rho(T) \sim T^\varepsilon$ for $x \cong 1$, which transforms into the dependence $\rho \sim -\ln T$ for $x \cong 0.9$, and finally, for $x=0.8$, exhibits a peak at ~ 7 K which is indicative of a quantum critical behavior for the NFL state setting in. In the compounds in this regime, a strong atomic disorder appears and leads to the spin-glass-like magnetic order, which modifies and complicates the understanding of the properties. A detailed study of this last factor, as well as the role of almost magnetic Rh $4d$ electrons provide an additional rationale for this work. Namely, we demonstrate the coexistence of a quantum critical behavior of $4f$ electrons with the presence of spin fluctuations due to $4d$ electrons and show that they differ essentially.

The structure of the paper is as follows. In Sec. II we provide experimental details of the synthesis and the measuring techniques. In Sec. III we present the magnetization data and provide the temperature dependence of the specific heat. Finally, in Sec. IV we discuss in detail the physical implications of the results and determine the main features of the phase diagram on the T - x plane.

II. EXPERIMENTAL DETAILS

Pure CeRhSb and CeRhSn samples were first prepared by arc melting of the weighted amount of each component. The dilute CeRhSb $_{1-x}$ Sn $_x$ alloys were then prepared by diluting nominal compositions of the master compounds. To ensure homogeneity, each sample was turned over and remelted several times and then annealed at 800 °C for 2 weeks. The samples were carefully examined by x -ray diffraction and found to be single phase (with the hexagonal structure of the Fe $_2$ P type, space group $P\bar{6}2m$). The single phase samples are possible to synthesize only in the $x \geq 0.78$ concentration range.

A standard four-terminal ac technique was used to measure the resistance of each sample.

The magnetic susceptibility was measured in the 1.9–300 K regime by use of a commercial ac Lake-Shore susceptometer. The amplitude of the excitation field was 1 mT at a fixed frequency of 10 kHz. dc susceptibility and the magnetization-curve measurements were carried out using a commercial SQUID magnetometer (Quantum Design) for temperatures in the range of 1.8–300 K.

Specific heat measurements have been performed in a fully adiabatic calorimeter between 2.7 K and 30 K.

III. ELECTRICAL RESISTIVITY AND MAGNETIC PROPERTIES FOR $x \geq 0.78$

In Fig. 1 we display the temperature dependence of the relative electrical resistivity $\rho(T)/\rho(300\text{ K})$ for the samples with $x \geq 0.82$. For CeRhSn and CeRhSb $_{0.04}$ Sn $_{0.96}$ the resistivity has a clear maximum at the temperature $T_{\text{max}} \cong 70\text{ K}$, below which the coherence effects appear, and the temperature power law T^ϵ dependence with exponent ϵ , which is strongly dependent on x . The resistivity $\rho(T)$ data displayed in Fig. 1 can be described by the relation $\rho(T)/\rho(300\text{ K}) = \sigma[1 + (T/T_0)^\epsilon]$, where σ , T_0 , and ϵ are adjustable parameters in the temperature range $T < 20\text{ K}$. The fitting procedure yields the value of $T_0 \cong 6\text{ K}$ and $\epsilon = 0.93, 0.65,$ and 0.63 , respectively, for the compounds with $x = 1, x = 0.98,$ and $x = 0.96$. The value of σ is a measure of the residual resistivity. The resistivity maximum is strongly reduced for the samples in the regime $0.82 < x < 0.9$ and the low-temperature $\rho(T)$ is almost constant. For the sample with $x = 0.82$ the maximum is slightly enhanced, while for T in the range from 8 to 20 K, $\rho \sim -\ln T$, and finally, saturates for $T < 8\text{ K}$. Details of the fitting procedure have been discussed already.⁷

In Fig. 2 we display the ac susceptibility χ under zero-field cooling (ZFC) versus temperature for the series CeRhSb $_{1-x}$ Sn $_x$ with $x \geq 0.78$. The $\chi(T)$ data exhibit two qualitatively different temperature dependences characteris-

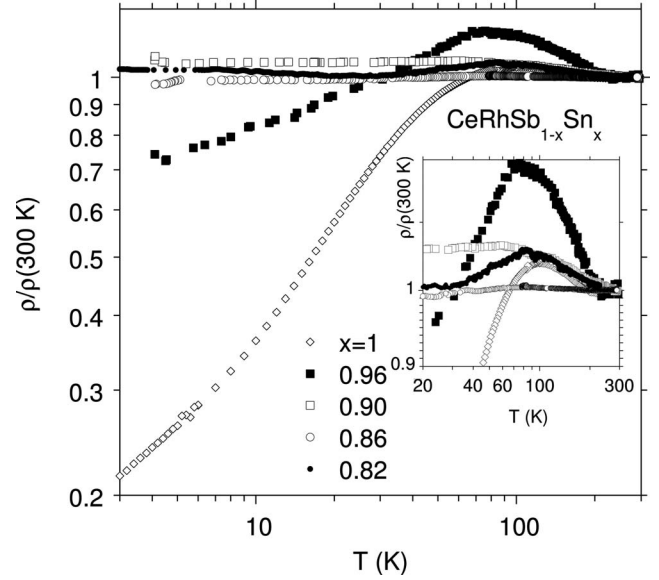


FIG. 1. Temperature dependence of the relative resistivity ρ for CeRhSb $_{1-x}$ Sn $_x$ system for $x > 0.80$. Inset, illustration of the gradual disappearance of the resistivity peak as x decreases.

tic for the samples displayed in Fig. 2(a) and Fig. 2(b), respectively. In Fig. 2(a) we show $\chi(T)$ for $0.8 \leq x \leq 1$; it follows a modified Curie-Weiss (CW) law in the temperature range $2 < T < 65\text{ K}$ and $\chi \sim T^{-n}$ below $\sim 6\text{ K}$.

The susceptibility of the samples $x \leq 0.8$ displayed in Fig. 2(b) show a cusplike maximum at $\sim 3\text{ K}$ (cf. the inset) characteristic for the magnetic phase transition, and the modified CW law between ~ 3.3 and 65 K . The ac susceptibility parametrizations for the CeRhSb $_{1-x}$ Sn $_x$ samples in the range $x \geq 0.78$ are collected in Table I. In Fig. 2(b) the ac susceptibility also exhibits a second maximum at about 120 K, suggestive of formation of the magnetic clusters, which is also confirmed by the dc susceptibility data obtained for CeRhSb $_{0.22}$ Sn $_{0.78}$ in magnetic field of 300 mT.

The dc susceptibility shown in Fig. 3 is hysteretic under zero-field and field cooling (FC) and also exhibits a knee-shaped phase transition at about 120 K (see the inset for details), which is very similar to that observed in PdFeMn,⁸ or LaFe $_7$ Al $_6$ (Ref. 9), and is indicative of a transition to an inhomogeneous magnet (mictomagnet). The inhomogeneous magnetic state may be understood as a mutually blocked assembly of ferromagnetic clusters.

The susceptibility in the higher-temperature regime contains a constant term χ_0 and the Curie-Weiss contribution. As we will discuss below, the χ_0 contribution comes from the Fermi-liquid component due to $4d$ electrons of Rh, whereas the CW part comes from $4f$ electrons, which form NFL at low T .

In our previous works (Refs. 10 and 11) we have discussed the possible origin of magnetism in these high-temperature ordered magnetic clusters. The magnetism can arise from either Rh clusters or Ce $4f$ electrons interacting with the Rh $4d$ and Sn conduction electrons. We note that the high-temperature magnetic phase transition exists only for the Sn-rich CeRhSb $_{1-x}$ Sn $_x$ compounds, and the ordering temperature strongly decreases with the increasing Sb content.

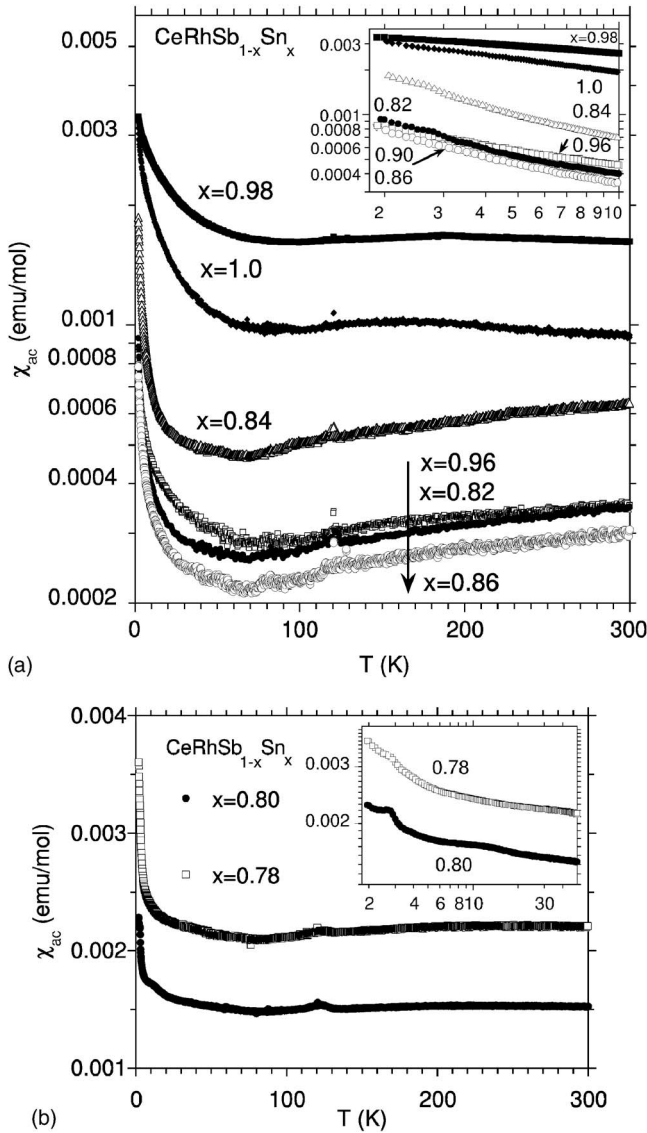


FIG. 2. Temperature dependence of the ac susceptibility for $\text{CeRhSb}_{1-x}\text{Sn}_x$ systems with $x=1, 0.98, 0.96, 0.90, 0.86, 0.84$, and 0.82 (a); and $x=0.80$, and 0.78 (b). A qualitative difference of $\chi(T=3\text{ K})$ behavior on panel (b) is attributed to the presence of the magnetic phase transition. Inset, (a) the scaling $\chi \sim T^{-m}$ on the double logarithmic scale below 10 K, and (b) the susceptibility in the log-log scale for $T < 70\text{ K}$. Note the cusp present below 5 K.

In Fig. 4 the magnetization curves for the sample $x=0.8$ for different T , are shown. Drawing of the Arrott plots turned out to be inconclusive; likewise, a fitting of the Brillouin curve with a variable spin was unsuccessful. The shape of M vs H plots at different temperatures exclude, in our view, a sizeable impurity contribution effect. Conversely, these curves rather represent a behavior of an itinerant magnet with a very small moment, originating from the competitive exchange interactions, since the curves do not saturate in the accessible field range up to 5 T. In Fig. 5 we plot M vs H/T . In the small-field regime, $M = \chi H$, so the scaling with H/T implies that $M = (\chi T)H/T$ and χT varies slowly with T . The deviation from the straight-line dependence would suggest the influence of a molecular field ($J_{\text{ex}}M$) on

the magnetic moments, because M should be a function of $H_{\text{eff}}/T = (H + J_{\text{ex}}M)/T$, where H_{eff} is the effective field and J_{ex} is the exchange integral.

The linear dependence and T -scaling of M vs H/T is observed for very small $H/T < 0.1\text{ T/K}$ region at $T \sim 5\text{ K}$. A very similar behavior was observed for the sample $\text{CeRhSb}_{0.22}\text{Sn}_{0.78}$.

IV. SPECIFIC HEAT: SPIN-FLUCTUATION VERSUS QUANTUM FLUCTUATION CONTRIBUTIONS

In Fig. 6 we plot the specific-heat C/T data versus T in the log-log scale. In the inset the specific heat data are displayed as $\Delta C/T$ versus T , where $\Delta C/T \equiv C/T(\text{CeRhSb}_{1-x}\text{Sn}_x) - C/T(\text{LaRhSn})$. By subtracting the heat capacity of pure LaRhSn we can observe a power-law increase of $\Delta C/T$ for temperatures $2 < T < 10\text{ K}$, which usually is taken as experimental evidence for a NFL behavior. Note that the subtracted LaRhSn contribution eliminates the contribution due to Ce, as the structure of the two systems is the same. The singular part of the specific heat can be parametrized by the dependence $\Delta C/T = bT^{-s}$ (cf. solid lines in the inset), with s and b listed in Table II.

By comparing the C/T curves with that for LaRhSn we see that the low- T increase must be due to the $4f$ Ce electrons, whereas the higher- T maximum is attributed to Rh $4d$ electrons, which contribute equally in all cases. This fact means also that the thermal fluctuations due to $4f$ -Ce and the $4d$ -Rh electrons are essentially decoupled as the corresponding maxima as well separated on the T scale.

We have also replotted C/T as a function of T^2 . A T^2 dependence in the temperature range 10–20 K provides the value of $\gamma_0 \equiv C(T \rightarrow 0)/T$ coefficient $\approx 60\text{ mJ/mol K}^2$ (see Table II), characteristic of correlated-electron behavior, here characterizing $4d$ electrons. Furthermore, the specific heat data in the range $6 \leq T \leq 25\text{ K}$ obey the relationship $C/T = \gamma^* + \delta T^2 \ln(T/T^*)$, representing a spin-fluctuation contribution $T^3 \ln(T/T^*)$ to the specific heat¹² (see also Fig. 7). Here γ^* is the linear coefficient enhanced by the mass-enhancement factor m^*/m_0 and T^* is the spin-fluctuation temperature.

The above equation also fits well the C/T data for LaRhSn in the temperature range 2–25 K, with the fitting parameters included in Table II. We also note, that for the temperatures $T > 6.5\text{ K}$, the same parameters, obtained for LaRhSn (Table II) fit well the C/T experimental data for CeRhSn and $\text{CeRhSb}_{1-x}\text{Sn}_x$, where $x \geq 0.78$, which strongly suggests that the high- T spin-fluctuation contribution comes from the Rh $4d$ electrons. In the low-temperature regime $T < 9\text{ K}$, C/T has the dependence T^{-s} (cf. also the fitting in Fig. 6 to $\Delta C/T$).

We emphasize, similar values of the exponent s are obtained irrespectively of the circumstance whether we take the data of C/T of the actual system or the data of $\Delta C/T$ with the background (LaRhSn) contribution subtracted (cf. Table II). This means again that the $4f$ -electron contribution to the NFL behavior is well separated from the spin-fluctuation contribution due to $4d$ electrons. In other words, in our CeRhSn system we have both the spin and the quantum fluc-

TABLE I. ac susceptibility parametrizations of the CeRhSb_{1-x}Sn_x samples.

CeRhSb _{1-x} Sn _x <i>x</i>	$\chi = \chi_0 + C/(T - \theta)$			$\chi = aT^{-m}$	
	χ_0 (emu/mol)	θ (K)	<i>C</i> (emu K/mol)	<i>a</i> (emu/mol)	<i>m</i>
1.00				3.77×10^{-3}	0.29
0.98				3.75×10^{-3}	0.16
0.96	2.60×10^{-4}	-2.74	2.52×10^{-3}	1.05×10^{-3}	0.37
0.90	2.30×10^{-4}	-2.46	2.00×10^{-3}	1.16×10^{-3}	0.54
0.86	1.98×10^{-4}	-0.69	1.53×10^{-3}	1.08×10^{-3}	0.51
0.84	2.42×10^{-4}	0.18	2.77×10^{-3}	2.90×10^{-3}	0.64
0.82	2.39×10^{-4}	-0.31	1.56×10^{-3}	1.29×10^{-3}	0.54
		1.9 < <i>T</i> < 65 K		<i>T</i> < 10 K	
0.80	14	-11.1	6.2		
0.78	21	-0.76	3.1		
		3.2 K < <i>T</i> < 65 K			

tuations present, albeit originating from different electronic subsystems. In principle, one can try to fit also the low-*T* (*T* < 6 K) data to the above spin-fluctuation formula for *C/T*. The result of such fitting is shown in Fig. 8. The fitted values of γ_f are in the range 180–260 mJ/mol K², a typical value for moderate heavy-fermion compound containing Ce. Nonetheless, the fit quality is somewhat poorer, particularly for *x* < 1, and also obeyed in a narrow temperature interval 2–6 K, whereas the fit to the law T^{-s} to $\Delta C/T$ is better and in a wider *T* range, 2–10 K. This is the reason why the NFL interpretation seems to be more proper. Nonetheless, the extension of the measurements to much lower temperatures would probably resolve this problem definitely. The subtlety of the difference in fitting either the spin-fluctuation formula (Fig. 8) or the critical behavior T^{-s} (Fig. 7) means that the 4*f* subsystem is on the brink of the HF-NFL instability.

We therefore conclude that two types of component quantum liquids appear in the CeRhSb_{1-x}Sn_x system: one repre-

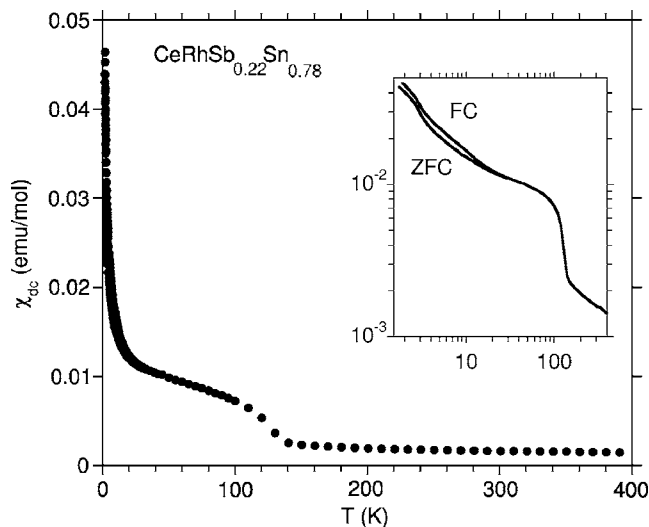


FIG. 3. Field-cooled and zero-field-cooled dc susceptibilities in the magnetic field of 300 Oe for CeRhSb_{0.22}Sn_{0.78}. Inset, detailed behavior for *T* < 100 K.

sents the low-temperature Ce contribution (absent in LaRhSn system), and another one, the higher-temperature Rh contribution. Our interpretation of the complicated ground state of CeRhSn in relation to other Ce-intermetallics with NFL behavior, has been recently discussed by the nuclear magnetic resonance (NMR) studies.¹⁴ Namely, the *T*-dependence of nuclear spin-lattice relaxation rate $1/T_1$ of Sn strongly suggests that the spin fluctuations are essential for low-energy excitations in CeRhSn below 10 K, whereas the macroscopic measurements exhibit NFL-like anomalies at low *T*'s down to 0.1 K.^{5,15} The magnetic instability observed in the ac magnetic susceptibility data was also discussed for CeRhSn in Ref. 16. Although the analysis of an interplay of the atomic disorder (discussed recently in, e.g., Ref. 17) and the spin fluctuations still remains open, the present specific heat re-

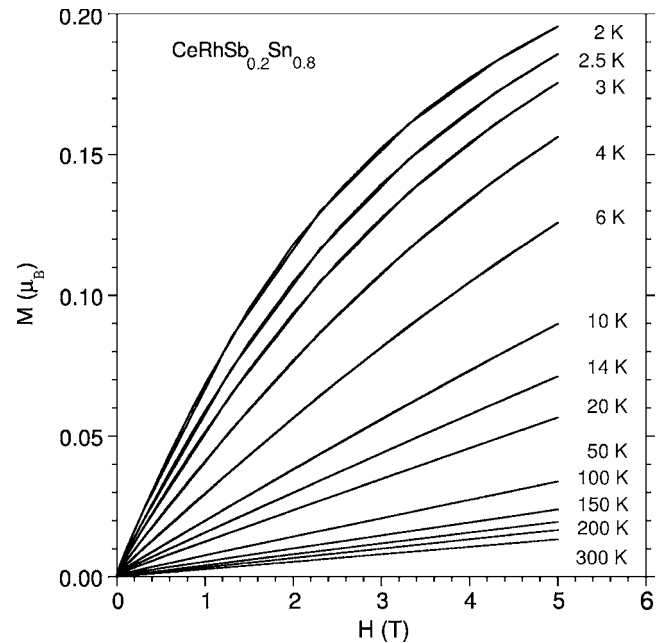


FIG. 4. Magnetization curves for the CeRhSb_{0.8}Sn_{0.2} sample in the *T* range 2–300 K.

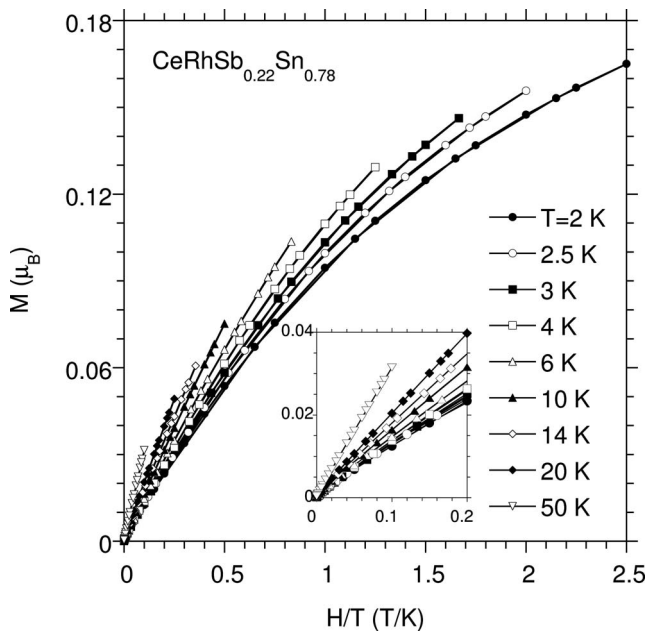


FIG. 5. Scaling of M data with H/T . The data are roughly convergent with $H \rightarrow 0$ and $T < 6$ K. Inset, details of the zero-field intercept.

sults suggest that CeRhSn is placed in the vicinity of the magnetic instability and has the NFL behavior. We are aware of the fact that such a *decomposition* of the system hybridized electrons into the Fermi-liquid ($4d$ electrons) and the non-Fermi ($4f$ electrons) components is probably approximate and facilitated by the presence of disorder.

It is evident (cf. Fig. 9) that the anomalous low- T contribution to the heat capacity C/T is dependent on applied magnetic field. The field-dependent upturn observed in the specific heat coefficient C/T is not typical for the Fermi-liquid

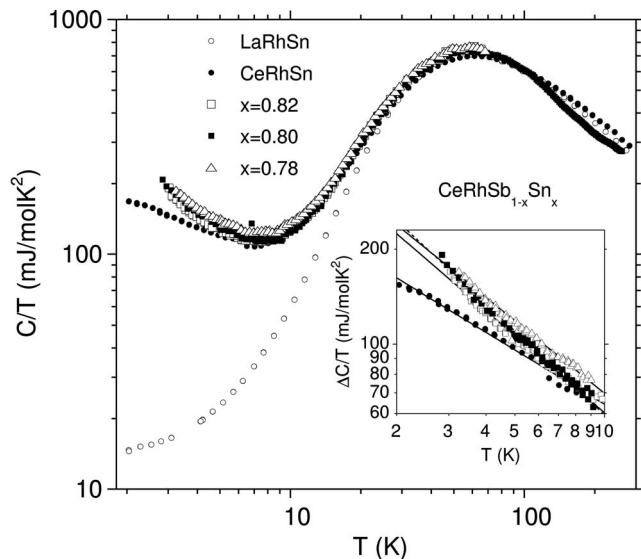


FIG. 6. Temperature dependence of the specific heat divided by temperature, $C(T)/T$. The inset shows $\Delta C(T)/T$ versus T , where $\Delta C = C(\text{sample}) - C(\text{LaRhSn})$. The critical behavior fitted in the inset (solid lines) is explained in the main text.

materials, where it is generally significantly suppressed by a strong magnetic field and is connected with the spin fluctuations suppression with the increasing field. However, some itinerant magnetic materials are known, for which the influence of magnetic field is quite varied (e.g., for Sc_3In C/T is enhanced for $H < 5$ T, while for $H > 5$ T the spin fluctuations are quenched).¹³ At present, this effect is not well understood. We only note that it cannot be related to metamagnetism, as the magnetization curves displayed in Fig. 4 are rather typical for a weak ferromagnet.

In the inset of Fig. 9 we plot the specific heat, C/T as a function of temperature for $\text{CeRhSb}_{0.18}\text{Sn}_{0.82}$. C/T has a sharp maximum at $T = 4.8$ K of the magnetic nature, indicative of another phase transition in the NFL metallic state (note, that the power-law exponents $\epsilon \rightarrow 0$ near the critical concentration $x \cong 0.8$ in the system $\text{CeRhSb}_{1-x}\text{Sn}_x$, see Fig. 1). A sharp feature in the specific heat data at ~ 4.8 K well may be correlated with the χ_{ac} corresponding cusp in the results displayed in Fig. 2. Such feature is also pronounced for the sample with $x = 0.78$ (cf. Fig. 3), but only in χ . From these results two conclusions can be drawn. First, an inhomogeneous type of magnetism coexists with the quantum fluctuations in the systems for $x \sim 0.8$. This, in turn, produces strongly x -dependent exponents dividing the systems into two classes: those with $x < 0.8$ and those with $x > 0.8$.

V. PHYSICAL DISCUSSION

In this paper we have analyzed the resistivity, the ac and dc susceptibilities, the magnetization curve, and the specific heat of the non-Fermi liquid metallic systems $\text{CeRhSb}_{1-x}\text{Sn}_x$, with $0.78 \leq x \leq 1$. On the basis of these results we have singled out both the spin-fluctuation contribution coming from the $4d$ electrons and the singular quantum-fluctuation part at the lowest temperatures due to Ce $4f$ electrons. The two processes can be separated, since the quantum fluctuations show a divergent behavior below 10 K, whereas the upturn in C/T due to the $4d$ spin fluctuations could become observable only for $T < 1$ K. This circumstance allowed us to differentiate between them. Those fluctuations still coexist with a weak and inhomogeneous magnetic order among itinerant electrons, presumably of $4f$ character. The presence of both magnetic and atomic disorder leads to a *nonuniversal*, i.e., to x -dependent critical exponents of both χ , C/T , and ρ .

On the basis of the experimental results analyzed in this paper, as well on our previous work,^{4,7} we can draw an overall schematic phase diagram for $\text{CeRhSb}_{1-x}\text{Sn}_x$ on the T - x plane and in the full x range; this is shown in Fig. 10. The existence of a low-moment state seems to be a universal feature of the whole metallic regime. This property is shared by both NFL and HF systems. Therefore, the appearance of the non-Fermi liquid phase must be related to specific features of electronic states, independent of whether the system is very weakly magnetic or paramagnetic. In other words, the *itinerant* nature of $4f$ electrons, but at the border of their localization, is the prerequisite of this singular quantum behavior for $T \rightarrow 0$. The role of quantum fluctuations leading to the non-Landau liquid behavior will be particularly enhanced if the reduced by the correlations kinetic energy of the f

TABLE II. CeRhSb_{1-x}Sn_x; b and s parameters for the best fits of an equation $\Delta C/T = bT^{-s}$ to the experimental data obtained for $T < 9$ K (see Fig. 6) and $C/T = bT^{-s}$ (see Fig. 7), and the Sommerfeld coefficient γ_0 obtained at $T=0$ from the linear dependence of C/T vs T^2 . The fitting parameters are obtained with an accuracy: $b \pm (3-7)$, $s \pm 0.01$, and $\gamma_0 \pm 1$. The parameters listed are also for the best fits of the equation $C/T = \gamma^* + \delta T^2 \ln(T/T^*)$ to the experimental data for $T > 6.5$ K (h), respectively. For LaRhSn the parameters were obtained from the corresponding fitting in the range 1.9–25 K.

x	b $\left(\frac{\text{mJ}}{\text{mol K}^2}\right)$	s $\frac{\Delta C}{T}$	s $\frac{C}{T}$	γ_0 $\left(\frac{\text{mJ}}{\text{mol K}^2}\right)$	γ^* $\left(\frac{\text{mJ}}{\text{mol K}^2}\right)$	δ $\left(\frac{\text{mJ}}{\text{mol K}^4}\right)$	T^* (K)
1	241	0.57	0.41	76	92.6 ± 1.4	0.15 ± 0.03	0.85 ± 0.03
0.82	394	0.81	0.74	66	85.0 ± 0.9	0.16 ± 0.03	0.71 ± 0.02
0.80	444	0.86	0.82	61	85.2 ± 1.2	0.16 ± 0.03	0.76 ± 0.02
0.78	407	0.78	0.71	76	94.1 ± 1.0	0.16 ± 0.03	0.66 ± 0.02
LaRhSn					13.3 ± 0.3	0.15 ± 0.01	0.43 ± 0.07

electrons becomes comparable to their characteristic energy due to magnetic interaction. Also, the instability of the systems in the concentration regime $0.2 < x < 0.78$ may be of *electronic origin*,¹⁹ since the magnetic and metallic phases are of competitive nature.

One should also note that the magnetic susceptibility shows here qualitatively similar divergence with $T \rightarrow 0$ (in the regime of measurements with $T < 10$ K), as the corresponding behavior of NFL on the Sb-rich side, $x \geq 0.12$.⁴ However, the resistivity maximum (at $T \sim 60$ – 80 K) almost disappears for $x < 0.9$. The presence of this resistivity maximum and the $-\ln T$ behavior accompanying it⁴ was ascribed

to the onset of f -electron delocalization when cooling the system. In other words, above $T = T_{\max}$ we have essentially the Kondo-type scattering, whereas below $T = T_{\max}$ the *coherence* of f states sets in and they become delocalized. Using the standard expression for the virtual bound state width,¹⁸ we obtain that $k_B T_{\max} \sim \pi V^2 \rho(\epsilon_F)$, where V is the magnitude of intra-atomic hybridization of f states with the conduction electrons and $\rho(\epsilon_F)$ is the density of states in the bare conduction band at the Fermi energy. Taking typical values $\rho(\epsilon_F) \sim 1/3$ (eV atom)⁻¹ and $V \sim 0.1$ eV, we obtain $T_{\max} \sim 100$ K, a correct order of magnitude. On the other hand, the effective f -electron bandwidth is of the order $T_K \sim 2(V^2/|\epsilon_f|)(1-n_f)$, where $|\epsilon_f| \sim 1$ – 2 eV is the bare f -level position and $(1-n_f) \sim 0.05$ is the deviation from Ce³⁺ valence. The above values provide the estimate of $T_K \sim 10$ K. The lower temperature (T_K) determines thus the nonmagnetic character of the correlated quantum liquid, which turns into either heavy Fermi liquid (HF) or non-Fermi liquid (NFL),

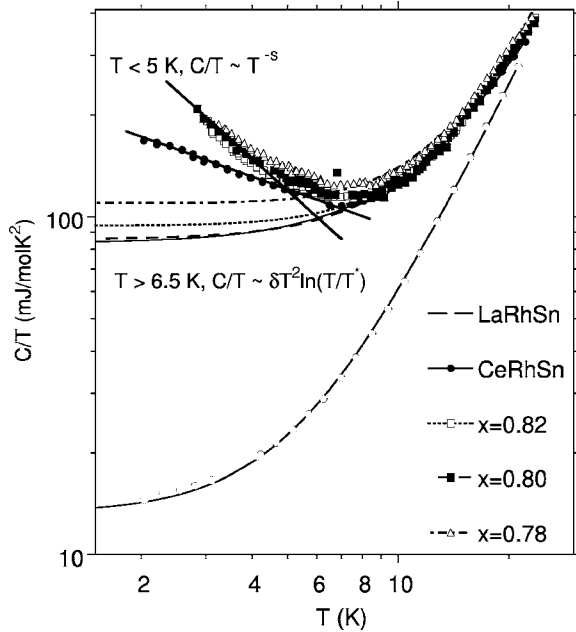


FIG. 7. The specific heat C/T data fitted to the spin-fluctuation formula $C/T = \gamma^* + \delta T^2 \ln(T/T^*)$ in the higher temperature ($6.5 < T < 23$ K) region. At low temperatures, $C/T \sim T^{-s}$ (the straight lines are the fits plotted in the log-log scale). The fitted curve for LaRhSn is also included for comparison. The straight lines for $T < 6$ K represent the power law dependences, whereas the flat parts below them are the extrapolation tails of the spin-fluctuation formula.

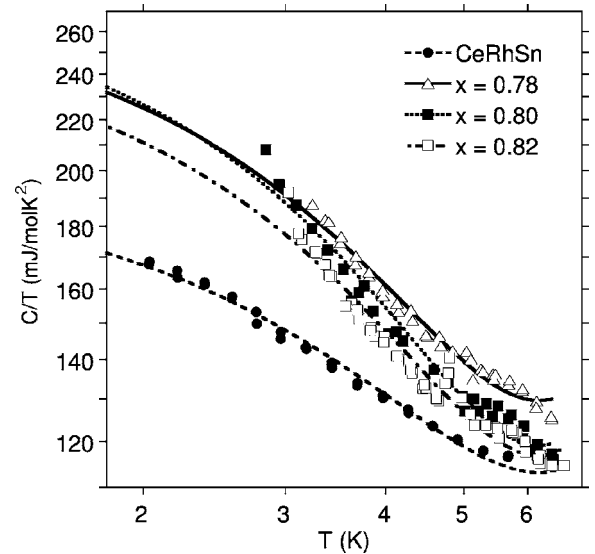


FIG. 8. The fitting as in Fig. 7 of the spin-fluctuation formula for C/T in the low- T range, $T < 6.5$ K. Note that the quality of this fit is not as good as in T^{-s} law in the foregoing picture.

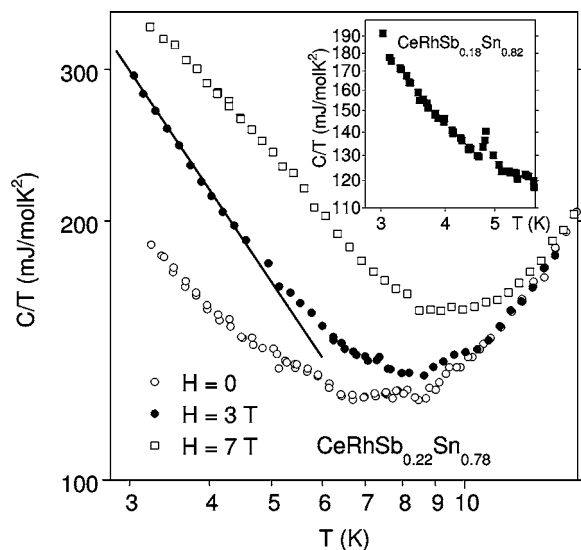


FIG. 9. C/T as a function of T for three values of applied magnetic field. Inset, C/T vs T for $\text{CeRhSb}_{0.18}\text{Sn}_{0.82}$ with a peak at $T \approx 4.7$ K. The straight line shows the fit to the power law dependence with the value of exponent $s=1$.

depending on whether the magnetic (exchange) interaction among f itinerant electrons (characterized as T_{RKKY}) are weaker or comparable to T_K , respectively. Also, the absence of well-defined resistivity maximum in Sn-rich samples may mean that the f -electrons are delocalized already in the regime $T < 100$ K. This feature distinguishes the behavior of the NFL state of CeRhSn (and of the samples in Sn-rich regime) from that near the transition to the Kondo insulator.⁴ Also, the intersite magnetic interactions, as seen by the values of Curie-Weiss temperature, are stronger in the NFL state. Such a difference may arise from the presence of $4d$ states due to Rh at the Fermi level [enhancing $\rho(\epsilon_F)$] only in the present case.

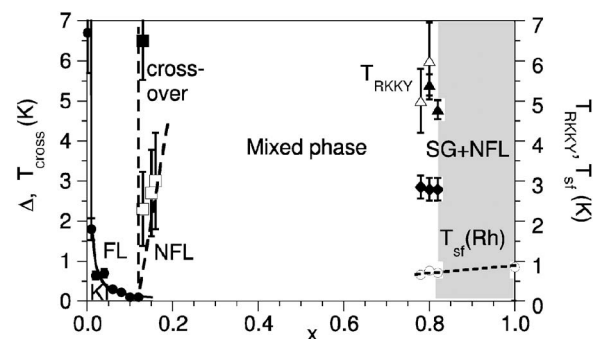


FIG. 10. Schematic phase diagram in the full concentration x -range. The part for $x \leq 0.2$ is reproduced from Ref. 4. On the right, $T_{sf}=T^*$ characterizes the spin-fluctuation temperature due to $4d$ electrons. Temperature T_{RKKY} is taken as the cusp temperature shown in Fig. 2(b) [open triangles mark the temperatures at which $M(H)$ deviates from linearity]. Full diamonds are extracted from $C(T)/T$ maximum. SG+NFL denotes a coexistence of an itinerant $4f$ electron spin-glass state with non-Fermi liquid behavior.

ACKNOWLEDGMENTS

The authors are grateful to John Mydosh for pointing out the possible importance of $4d$ electrons due to rhodium. Two of the authors (A.Ś. and M.G.) acknowledge the support of the State Committee for Scientific Research (KBN), through the Grant No. 1 P03B 052 28. One of the authors (J.S.) acknowledges the Polish Foundation for Science for the years 2003–2006 and for the Grant No. 1 P03B 001 29 of the Ministry of Education and Science. This work was partly supported by Scientific Network *Mag-El-Mat* and the COST P-16 European Network entitled “*Emergent Behaviour in Correlated Matter*.” The authors thank also Dariusz Kaczorowski for his help and critical remarks.

¹S. K. Malik and D. T. Adroja, Phys. Rev. B **43**, 6277 (1991).

²T. Takabatake, G. Nakamoto, H. Tanaka, Y. Bando, H. Fujii, S. Nishigori, H. Goshima, T. Suzuki, T. Fujita, I. Oguro, T. Hiraoka, and S. K. Malik, Physica B **199-200**, 457 (1994); S. K. Malik, Latika Menon, V. K. Pecharsky, and K. A. Gschneidner, Jr., Phys. Rev. B **55**, 11471 (1997).

³J. Spalek and R. Doradziński, in *Magnetism and Electronic Correlations in Local-Moment Systems: Rare Earth Elements and Compounds*, edited by M. Donath, P. A. Dowben, and W. Nolting (World Scientific, Singapore, New Jersey, London, Hong Kong, 1998), p. 387; R. Doradziński and J. Spalek, Phys. Rev. B **58**, 3293 (1998); for brief review see: J. Spalek and R. Doradziński, Acta Phys. Pol. A **96**, 677 (1999); **97**, 71 (2000).

⁴A. Ślebarski and J. Spalek, Phys. Rev. Lett. **95**, 046402 (2005); J. Spalek, A. Ślebarski, J. Goraus, L. Spalek, K. Tomala, A. Zarzycki, and A. Hackemer, Phys. Rev. B **72**, 155112 (2005).

⁵A. Ślebarski, A. Jezierski, M. B. Maple, and A. Zygmunt, Acta Phys. Pol. B **32**, 3331 (2001); A. Ślebarski, M. B. Maple, E. J.

Freeman, C. Sirvent, M. Radłowska, A. Jezierski, E. Granado, Q. Huang, and J. W. Lynn, Philos. Mag. B **82**, 943 (2002); P.-C. Ho, V. S. Zapf, A. Ślebarski, and M. B. Maple, Philos. Mag. **84**, 2119 (2004).

⁶R. B. Griffiths, Phys. Rev. Lett. **23**, 17 (1969); A. H. Castro Neto, G. Castilla, and B. A. Jones, *ibid.* **81**, 3531 (1998).

⁷A. Ślebarski, T. Zawada, J. Spalek, and A. Jezierski, Phys. Rev. B **70**, 235112 (2004); for a detailed analysis of the resistivity for $x \rightarrow 0$ see A. Ślebarski, T. Zawada, and J. Spalek, Physica B **359-361**, 118 (2005).

⁸B. H. Verbeek, G. J. Nieuwenhuys, H. Stocker, and J. A. Mydosh, Phys. Rev. Lett. **40**, 586 (1978).

⁹T. T. M. Palstra, G. J. Nieuwenhuys, J. A. Mydosh, and K. H. J. Bushow, Phys. Rev. B **31**, 4622 (1985).

¹⁰A. Ślebarski, M. Radłowska, T. Zawada, M. B. Maple, A. Jezierski, and A. Zygmunt, Phys. Rev. B **66**, 104434 (2002).

¹¹A. Ślebarski, A. Czopnik, A. Zygmunt, and T. Zawada, J. Phys.: Condens. Matter **16**, 4897 (2004).

- ¹²S. Doniach and S. Engelsberg, Phys. Rev. Lett. **17**, 750 (1966).
- ¹³K. Ikeda and K. A. Gschneidner, Jr., J. Magn. Magn. Mater. **22**, 207 (1981).
- ¹⁴H. Tou, M. S. Kim, T. Takabatake, and M. Sera, Phys. Rev. B **70**, 100407(R) (2004).
- ¹⁵M. S. Kim, Y. Echizen, K. Umeo, S. Kobayashi, M. Sera, P. S. Salamkha, O. L. Sologub, T. Takabatake, X. Chen, T. Tayama, T. Sakakibara, M. H. Jung, and M. B. Maple, Phys. Rev. B **68**, 054416 (2003).
- ¹⁶A. Ślebarski, K. Grube, R. Lortz, C. Meingast, and H. v. Löhneysen, J. Magn. Magn. Mater. **272-276**, 234 (2004).
- ¹⁷A. Ślebarski, K. Szot, M. Gamża, H. J. Penkalla, and U. Breuer, Phys. Rev. B **72**, 085443 (2005).
- ¹⁸P. W. Anderson, Phys. Rev. **124**, 41 (1961); A. C. Hewson, *The Kondo Problem to Heavy Fermions* (Cambridge University Press, Cambridge, 1993), Chaps. 1 and 7.
- ¹⁹S. Kaprzyk (private communication).